Site-Specific Hydrogen-Bonding Interaction between *N*-Acetylproline Amide and Protic Solvent Molecules: Comparisons of IR and VCD Measurements with MD Simulations

Kwang-Im Oh,[†] **Jaebeom Han,**[†] **Kyung-Koo Lee,**[†] **Seungsoo Hahn,**[†] **Hogyu Han,**[‡] **and Minhaeng Cho*,**[†]

Department of Chemistry and Center for Multidimensional Spectroscopy, Korea University, Seoul 136-701, Korea

The effects of solute−solvent interactions on solution structures of small peptides have been paid a great deal of attention. To study the effect of hydrogen-bonding interactions on peptide solution structures, we measured the amide I IR and VCD spectra of *N*-acetylproline amide (AP) in various protic solvents, i.e., D_2O, MeOD, EtOD, and PrOD, and directly compared them with theoretically simulated ones. The numbers of protic solvent molecules hydrogen-bonded to the two peptide bonds in the AP were quantitatively determined by carrying out the molecular dynamics (MD) simulations and then compared with the spectral analyses of the experimentally measured amide I bands. The two peptides in the AP have different propensities of forming H-bonds with protic solvent molecules, and the H-bond population distribution is found to be strongly site-specific and solvent-dependent. However, it is found that adoption of the polyproline II (P_{II}) conformation by AP in protic solvents does not strongly depend on the hydrogen bond network-forming ability of protic solvents nor on the solvent polarity. We present a brief discussion on the validity as well as limitation of the currently available force field parameters used for the present MD simulation study.

I. Introduction

Recently, we showed that the aqueous solution structure of *N*-acetylproline amide (AP, Ac-Pro-ND$_2$, Figure 1) is close to an extended left-handed polyproline II (P_{II}) form.[1] The P_{II} conformation of aqueous AP was indicated by the infrared (IR) and vibrational circular dichroism (VCD) spectra of AP in liquid D_2O and their direct comparison with numerically simulated ones obtained using the *ff*03 force field[2] in the *AMBER 8* suite of programs.[3] These experimental and simulation results were found to be interesting when considering the recent experimental studies on molecular structures of alanine dipeptide (Ac-Ala-NHCH$_3$) in water.[4−8] By employing a variety of experimental techniques such as infrared absorption,[7] nonresonant Raman scattering, VCD, and two-dimensional (2D) vibrational spectroscopy,[4,6] the aqueous solution structure of the alanine dipeptide has been found to be P_{II}-like.

Despite the experimental suggestion of the P_{II}-like conformer for alanine dipeptide in liquid water, there still exist controversies over the driving force for stabilizing its P_{II} conformer in liquid water. The quantum chemistry calculations for alanine dipeptide in the gas phase suggested that the C_7 conformer is the most stable one because of its intramolecular hydrogen-bond formation.[9−13] Consistent with this result, it was suggested that alanine dipeptide adopts the C_7 conformation when dissolved in less polar aprotic solvents such as CDCl$_3$ that lack the ability to form hydrogen bonds with carbonyl oxygen atoms of a dipeptide.[14,15] On the other hand, if a dipeptide is surrounded by water molecules in an aqueous solution, it was conjectured that their strong hydrogen-bond formation with the peptides
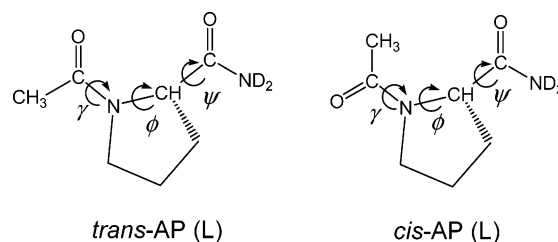
Figure 1. Chemical structures of trans-AP ($\gamma = 180°$) and cis-AP ($\gamma = 0°$) in L-form. Its secondary structure is determined by the two dihedral angles ϕ and ψ. L-Form AP was considered for all theoretical calculations unless otherwise noted in Figures 3, 4, 6, and 8.

would alter the dipeptide structure significantly from that in the gas phase.[16−22] One of the first theoretical investigations was performed by Han et al.,[23] where they carried out density functional theory (DFT) calculations for alanine dipeptide with four water molecules allowed formation of strong H-bonds with it. Their observation that two short water bridges connecting intrapeptide hydrogen-bond donor and acceptor groups are the major factor in stabilizing the P_{II} conformer in comparison to other conformers triggered a few related investigations. Recently, however, Pappu and co-workers suggested that the specific water−peptide interactions are not the dominant factor for stabilizing the P_{II} conformer of alanine dipeptide in water, but rather, the steric effect is.[24] That is, the determining factor for such a conformational preference is the consequence of minimizing intrapeptide steric conflicts. The role of solvent water molecules in this case is to screen the intrapeptide electrostatic (Coulombic) interaction. To address this issue, it is believed that the AP molecule can be an alternative interesting model system.[25] Unlike other dipeptides, AP has no amide H-atom in the acetyl-end peptide due to its five-membered pyrrolidine ring (see Figure 1) so that one of the two water

* To whom correspondence should be addressed: mcho@korea.ac.kr.
† Department of Chemistry and Center for Multidimensional Spectroscopy.
‡ Department of Chemistry.

bridges found in refs 5 and 23 is not allowed intrinsically. Nevertheless, AP can still form a water-assisted H-bond network, since the amide H-atoms in the amide-end peptide group ($-CONH_2$) are available for such network-forming water bridges. Then, a question is immediately raised. If solvent molecules can make hydrogen-bonding interactions with a solute peptide but they are not a good H-bond network-forming liquids, can they still be effective in stabilizing the P_{II} conformer of dipeptides? One can address this question by replacing water with methanol, ethanol, and propanol, which are all protic solvents but are gradually less effective in forming such H-bond networks in solutions compared to water. In addition, as the solvent changes from water, methanol, ethanol, to propanol, the volume of the chemical group attached to the hydroxyl group increases. Consequently, one can expect a progressive change in the solvation structure around the dipeptide due to the steric hindrance between the aliphatic groups of solvents. In relation to this phenomenon, we studied *N*-methylacetamide (NMA) in methanol solution and compared the result with that for NMA in liquid water (D_2O).[26,27] The number of methanol molecules H-bonded to the carbonyl oxygen atom of NMA varies from 1 to 2. Since a single H-bond with the carbonyl group induces an amide I mode frequency shift of about 20 cm^{-1} in the IR absorption spectrum, the NMA in methanol solution exhibits two frequency-resolved peaks. These two peaks are associated with two distinguished solvation structures that are different from each other by the number of methanol molecules H-bonded to the C=O group in the NMA. One can then expect that, in the case of AP in solution, the same spectral change would occur when the solvent water is replaced with methanol and other larger alcohols.

Thus, the main goals of the present investigation are to study the effect of hydrogen-bonding interactions on the AP conformation in solution by employing various protic solvents. IR and VCD spectroscopy and the computational method combining quantum chemistry calculation and molecular dynamics simulation are used to achieve these goals. Direct comparisons between experiments and theoretical results suggest that, regardless of the hydrogen bond network-forming ability of a given protic solvent and the solvent polarity, the AP dipeptide mainly adopts the P_{II} conformation in protic solvents. However, the H-bond distributions around the two carbonyl groups in the AP are site-specific and appear to be fairly different depending on the solvent. A detailed discussion and interpretation will be provided in this paper, then.

II. Experimental Section

In ref 1, we have already presented a detailed experimental procedure on how to prepare the L- and D-forms of *N*-acetylproline amide molecules. Thus, the IR and VCD spectroscopic measurements will be briefly outlined in this section.

IR and VCD spectra were measured on a Chiral*ir* FT-VCD spectrometer from Bomem/BioTools. This spectrometer is equipped with a HgCdTe detector having a cutoff at 8 cm^{-1} and a ZeSe photoelastic modulator (PEM) to create left and right circularly polarized radiation. The PEM was optimized for maximum quarter-wave response at 1400 cm^{-1}. To exchange the labile hydrogen atoms in AP for deuterium atoms, the peptide/D_2O solution was lyophilized twice on a SpeedVac (ThermoSavant), and subsequently, it was dissolved in D_2O or deuterated alcohols such as CH_3OD, C_2H_5OD, and CH_3CH_2-CH_2OD to a concentration of about 50 mg/mL. VCD and IR spectra were measured with a resolution of 4 cm^{-1} using a CaF$_2$ cell with a path length of 25 μm, and the sample cell chamber

TABLE 1: Atom Types in Propanol

atom	type	description
carbon	CT	sp^3 carbon atom
oxygen	OH	sp^3 oxygen atom in the hydroxyl group
hydrogen	HO	H atom in the hydroxyl group
	HC	H atom attached to the aliphatic carbon with no electron-withdrawing substituent
	H1	H atom attached to the aliphatic carbon with a single electron-withdrawing substituent

was purged with dehydrated N_2 gas to remove water vapor inside the chamber. Temperature of the sample cell was controlled with a circulating water bath (Sam Heung Instrument SH−R−WB10), and a temperature sensor was directly attached to the cell surface. All spectra were recorded at 10 °C. VCD spectra were collected in blocks for a total collection time of approximately 12 h (32 688 ac scans and 600 dc scans collected in 12 blocks) depending on the peptide sample investigated. The VCD baseline correction was made with both D- and L-AP spectra measured separately.

III. Molecular Dynamics Simulation Results

As discussed in detail in ref 1, one can use the molecular dynamics (MD) simulation method in combination with quantum chemistry calculation results to numerically simulate the IR and VCD spectra of AP in protic solvents. Although the conformational fluctuation of AP in solution can be studied by the MD simulation, the transition electric and magnetic dipoles, amide I local mode frequencies, and vibrational coupling constants should be determined as functions of the three dihedral angles γ, ϕ, and ψ, and they all were obtained by DFT using the *Gaussian 03* program at the B3LYP/6-311++G** level.[28]

A. MD Simulation Method. For both trans- and cis-AP in L-form (Figure 1), a series of MD simulations have been performed by using the *AMBER 8* program[3] with the force field parameter *ff*03[2]; note that the *ff*03 parameters, unlike *ff*99, were obtained by carrying out ab initio calculations with an implicit continuum solvent model. The composite system consists of a single trans-AP (cis-AP) molecule and 740, 725, 685, or 332 (794, 721, 686, or 325) D_2O, MeOD, EtOD, or PrOD molecules, respectively. For D_2O, we used the *ff*03 force field parameters in the *AMBER 8* program as described.[1] For methanol, we used the force field parameters in the *AMBER 8* program. The electrostatic partial charges of ethanol are available in ref 29. The bond lengths, angles, and van der Waals parameters of ethanol were reported in ref 30. However, the force field parameters for propanol are not available, so we have carried out appropriate quantum chemistry calculations by following the procedure provided in ref 30. We calculated various propanol conformations with the *Gaussian 03* suite of program, and used *espgen* and *respgen* methods in the *AMBER* program to determine the set of force field parameters for propanol. The atom types are summarized in Table 1, and the bond, angle, torsion, van der Waals, and partial charge parameters of propanol are given in Table 2 and Figure 2.[30] To run MD simulations, a periodic boundary condition was employed and the particle mesh Ewald summation method was used.[31] Each system was equilibrated for a few nanoseconds at 298 K (and 400 K) by using the Berendsen coupling algorithm[32] in a constant temperature condition. The production run was done for 3 (or more) ns at a given temperature. We found that the densities of D_2O, MeOD, EtOD, and PrOD at room temperature are 1.107, 0.813, 0.801, and 0.804 g/mL, respectively.

B. Conformational Analysis of AP in Protic Solvents: MD Simulation Results. From the explicit solvent MD trajectory

Site-Specific H-Bonding Interaction

J. Phys. Chem. A, Vol. 110, No. 50, 2006 **13357**

TABLE 2: Force Field Parameters for Propanol[30] [a]

Bond Parameters		
bond	K_r [b]	r_{eq} [c]
CT-CT	310.0	1.526
CT-H1	340.0	1.090
CT-HC	340.0	1.090
CT-OH	320.0	1.410
HO-OH	553.0	0.960

Angle Parameters		
angle	k_θ [d]	θ_{eq} [e]
CT-CT-CT	40.0	109.5
CT-CT-H1	50.0	109.5
CT-CT-HC	50.0	109.5
CT-CT-OH	50.0	109.5
CT-OH-HO	55.0	108.5
H1-CT-H1	35.0	109.5
H1-CT-OH	50.0	109.5
HC-CT-HC	35.0	109.5

Torsion Parameters				
torsion	no. of paths	$V_n/2$ [f]	γ [g]	n [h]
X-CT-CT-X	9	1.40	0.0	3.0
X-CT-OH-X	3	0.50	0.0	3.0

van der Waals Parameters		
atom type	$R*$ [i]	ϵ [j]
CT	1.9080	0.1094
H1	1.3870	0.0157
HC	1.4870	0.0157
HO	0.0000	0.0000
OH	1.7210	0.2104

[a] Atom types are listed in Table 1. [b] kcal/(mol Å²). [c] Å. [d] kcal/(mol radian²). [e] deg. [f] Magnitude of torsion in kcal/mol. [g] Phase offset in def. [h] The periodicity of the torsion. [i] van der Waals radius $R*$ for a given atom in Å. [j] van der Waals well depth for a given atom in kcal/mol.
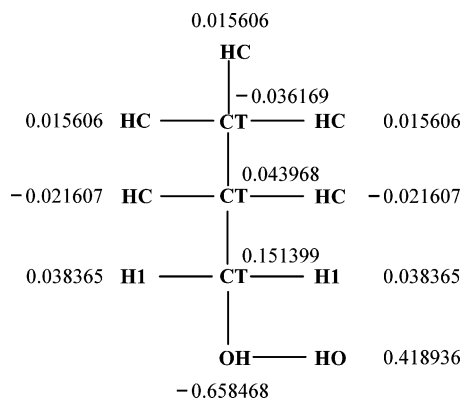
Figure 2. Atom types and partial charges for propanol considered in this study according to section III. A.

at 400 K, the distributions of the two dihedral angles ϕ and ψ for both rotamers (trans- and cis-AP) were obtained and plotted in Figure 3. It should be noted that the only reason for high-temperature MD simulation is to make the AP explore a broader range of conformational phase space. However, when we calculate the system−bath interaction-induced fluctuations of vibrational frequencies and perform the ensemble averaging, the room-temperature simulation trajectory was used. In Figure 3, the ϕ and ψ angle distributions of trans-AP are almost identical to those of cis-AP, and surprisingly, these distributions do not strongly depend on the details of solvent molecules and the solvent polarity. From these MD simulation results, one might conclude that the *ff*03 force field simulation predicts that the predominant conformations of trans- and cis-AP in all protic

solvents are close to the extended P_{II} form; note that the *ff*03 force field simulation of AP in D_2O solution also predicted that the AP structure is P_{II} (see the solid curves in Figure 3). The dominant P_{II} conformation of AP is not strongly dependent on the solvent polarity nor on the solvent dielectric property. Later in this paper, we will compare the predicted AP structures in protic solvents with those deduced from the analyses of the experimentally measured IR and VCD spectra.

C. Equilibrium H-Bond Population: Its Site Dependency. To quantitatively determine the number of solvent molecules that are H-bonded to either the acetyl-end or amide-end carbonyl oxygen atom, it is necessary to establish the set of H-bonding criteria for each protic solvent. Since the L-AP can exist in two different rotamers (trans and cis forms) in protic solvents, we need to separately consider the two cases for such a purpose. We first calculated the atom−atom radial distribution function, $g(r)$, between the H-bond donor (deuterium atom of the solvent OD group) and the H-bond acceptor (carbonyl oxygen atom of AP). Then, the first minimum (the first solvation shell) of $g(r)$ can be assumed to be the threshold distance for an H-bond, $r*$. In Table 3, these $r*$ values are summarized. Note that the H-bond threshold distance $r*$ of the acetyl-end peptide can be different from that of the amide-end peptide as shown in the AP-MeOD solution. It is found that the threshold distance $r*$ slightly increases as the solvent size increases from D_2O to PrOD; note that the first maximum position of $g(r)$ is little dependent on the size of alkyl groups. Now, the angle criterion for the H-bond is 120°, meaning that, when the angle of (AP)O···D−O(R) with R = D, Me, Et, or Pr is larger than 120°, the AP and solvent molecules are considered to be H-bonded to each other. Using these criteria, we have analyzed the MD trajectories and calculated the H-bond populations in detail.

In Figure 4, the populations of AP molecules with n H-bonded solvent molecules at the acetyl- and amide-end carbonyl oxygen atoms are separately plotted for trans- and cis-AP (see Table 4 for quantitative information). In the case of trans-AP in D_2O, the probability of finding the acetyl-end carbonyl oxygen atom with two H-bonded water molecules is 68.5%. On the other hand, that with no H-bonded water molecule is just about 0.7%. This means that the acetyl-end peptide group almost always interacts with one or two water molecules; note that, even though the probability of finding the peptide group with even three H-bonded water molecules is about 5−7%, we will ignore these species throughout this paper. In comparison to the acetyl-end peptide, however, the amide-end peptide is notably less exposed to solvent water molecules. More specifically, the populations of trans-AP molecules with zero, one, and two D_2O molecules H-bonded to the amide-end carbonyl group are 2.4%, 41.6%, and 56.0%, respectively. The asymmetric distribution of H-bonded water molecules in the two peptides is related not only to the difference in the chemical structures of the two peptides but also to the different charge distributions of the carbonyl oxygen atoms. From the DFT calculation for trans-AP in P_{II} conformation and ChelpG charge analysis,[33] the partial charge of the acetyl-end carbonyl oxygen atom is −0.6734e, whereas that of the amide-end carbonyl oxygen atom is −0.6400e. As will be shown below, this asymmetry of the H-bond populations at the two H-bonding sites appears to be general for all the protic solvents studied in this work.

If D_2O is replaced with MeOD, the H-bond population distributions at the two peptide sites dramatically change. For trans-AP in MeOD, the most probable solvation structure is the case when the acetyl-end carbonyl oxygen forms a *single* H-bond with a MeOD molecule. Similarly, the amide-end
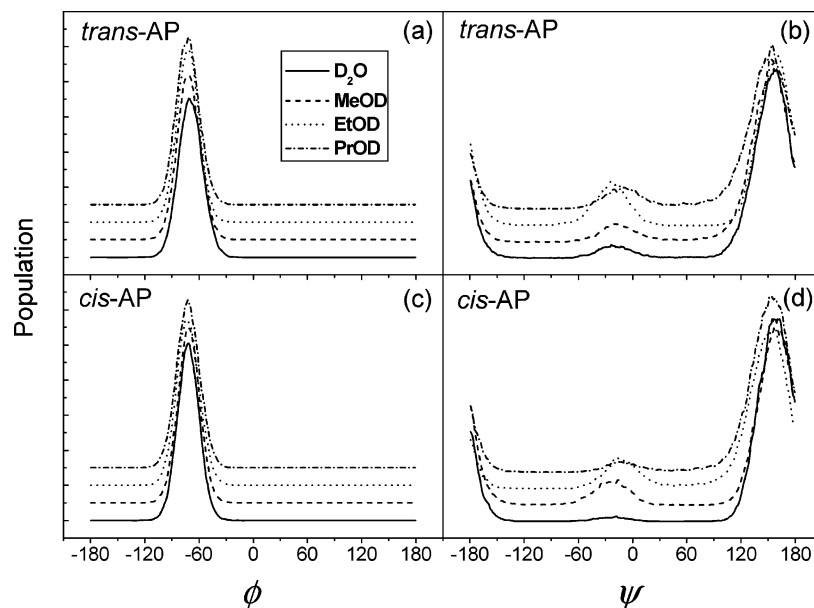
Figure 3. Population distributions of ϕ and ψ dihedral angles for trans- and cis-AP in protic solvents. Here, we used the 3 ns 400 K MD simulation (with the *ff*03 parameters) results obtained according to section III. A. These ϕ and ψ distributions indicate the conformations of AP in protic solvents are close to P_{II}.
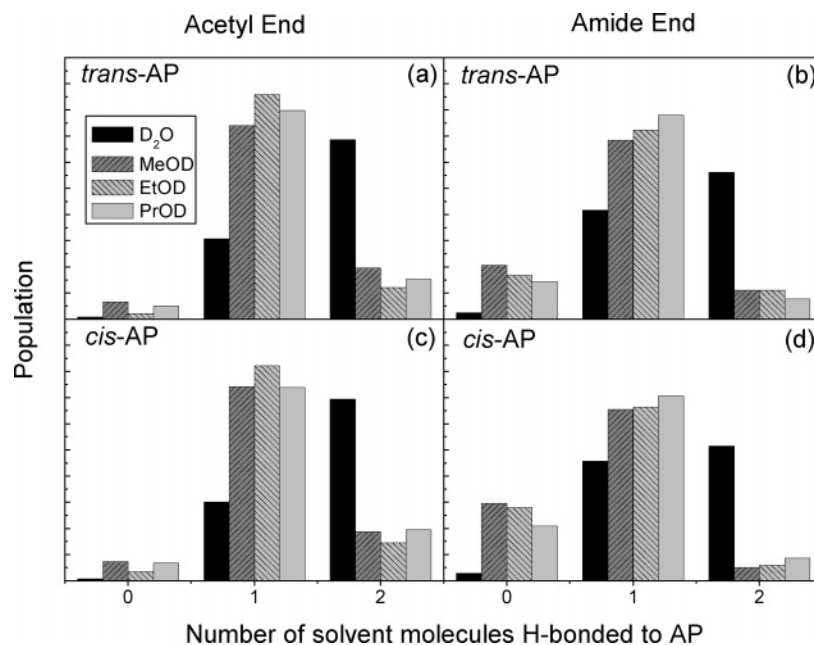
Figure 4. Population distributions of the numbers (N_{Ac} and N_{Am}) of solvent molecules H-bonded to the acetyl-end and amide-end peptides of trans-AP and cis-AP. We used the MD simulation results obtained according to section III.A. For quantitative information, see Table 4.

carbonyl group can mostly form a single H-bond with MeOD. The probability of finding carbonyl oxygen atoms of AP with two H-bonded MeOD molecules is relatively small in comparison to that with one H-bonded MeOD molecule. Since the MeOD solvent can make a relatively weak H-bond network around the solute AP, there is little chance for MeOD molecules to form a MeOD···MeOD bridge within the first solvation shell so that the number of MeOD molecules H-bonded to the carbonyl group of AP decreases in comparison to the case of solvent water. One may conjecture that the electrostatic (H-bonding) interaction strength between MeOD and C=O is weak in comparison to that between D_2O and C=O. However, it is known that the solvatochromic frequency shift of the amide I band induced by a single H-bonding interaction with MeOD is quantitatively similar to that with D_2O. This suggests that the H-bond strength in MeOD···O=C group is quantitatively similar

TABLE 3: Hydrogen Bond Threshold Distance r^* for trans- and cis-AP as Described in Section III. C^a

	threshold distance r^* (Å)			
	D_2O	MeOD	EtOD	PrOD
trans-AP	2.5	Ac: 2.7	2.8	2.8
	(1.8)	Am: 2.8	(1.8)	(1.8)
		(1.8)		
cis-AP	2.5	Ac: 2.7	2.8	2.9
	(1.8)	Am: 2.8	(1.8)	(1.8)
		(1.8)		

[a] Note that the r^* of the acetyl-end peptide slightly differs from that of the amide-end peptide in the AP−MeOD solution. The first maximum position of the radial distribution function $g(r)$ is in parentheses.

to that in DOD···O=C group. Another possible explanation for the above observation is that the methyl group in MeOD is

TABLE 4: Percent Probabilities of Finding [N_{Ac}, N_{Am}]$_{solvent}$ Species Obtained from the MD Simulation Trajectory Analyses for trans- and cis-AP as Described in Section III. C[a]

	Solvent D$_2$O							
rotamer	trans-AP				cis-AP			
			N_{Am}					
N_{Ac}	0	1	2	sum	0	1	2	sum
0	0.02	0.30	0.40	**0.72**	0.02	0.31	0.35	**0.68**
1	0.73	12.8	17.2	**30.7**	0.86	13.7	15.4	**30.0**
2	1.64	28.5	38.4	**68.5**	1.99	31.6	35.6	**69.2**
sum	**2.39**	**41.6**	**56.0**	**100**	**2.87**	**45.6**	**51.4**	**100**

	Solvent MeOD							
rotamer	trans-AP				cis-AP			
			N_{Am}					
N_{Ac}	0	1	2	sum	0	1	2	sum
0	1.34	4.43	0.71	**6.48**	2.13	4.72	0.36	**7.21**
1	15.2	50.6	8.16	**74.0**	21.9	48.5	3.74	**74.1**
2	4.03	13.4	2.15	**19.6**	5.52	12.2	0.94	**18.7**
sum	**20.6**	**68.4**	**11.0**	**100**	**29.6**	**65.4**	**5.04**	**100**

	Solvent EtOD							
rotamer	trans-AP				cis-AP			
			N_{Am}					
N_{Ac}	0	1	2	sum	0	1	2	sum
0	0.35	1.50	0.23	**2.08**	0.93	2.21	0.19	**3.33**
1	14.4	62.0	9.48	**85.9**	22.9	54.4	4.79	**82.1**
2	2.02	8.73	1.33	**12.1**	4.05	9.61	0.85	**14.5**
sum	**16.8**	**72.2**	**11.0**	**100**	**27.9**	**66.2**	**5.83**	**100**

	Solvent PrOD							
rotamer	trans-AP				cis-AP			
			N_{Am}					
N_{Ac}	0	1	2	sum	0	1	2	sum
0	0.73	3.97	0.39	**5.09**	1.40	4.74	0.58	**6.72**
1	11.4	62.1	6.13	**79.6**	15.4	52.1	6.34	**73.8**
2	2.18	11.9	1.17	**15.3**	4.04	13.7	1.66	**19.4**
sum	**14.3**	**78.0**	**7.69**	**100**	**20.8**	**70.5**	**8.58**	**100**

[a] The boldface values are used to plot Figure 4.

simply larger in volume than just a single D atom in D$_2$O, so that the steric effect plays a role in making such a difference in the H-bond population distributions.

Now, it is interesting to note that, as the size of solvent molecules increases further to EtOD and PrOD, the probability of finding AP molecules with no H-bonded EtOD or PrOD at each peptide site does not change much. In addition, the overall H-bond population distributions around the two peptides of AP in EtOD and PrOD are very similar to that in MeOD (see Figure 4). Thus, it is believed that, even though the steric effect is the key factor for determining the H-bond population distribution, it is quantitatively similar as long as the chemical group varies from Me to Pr. For the series of AP solutions considered in this paper, we find that the order of the steric effect on H-bonding propensity is D$_2$O < MeOD ≈ EtOD ≈ PrOD.

Although we presented MD simulation results on the H-bond population distributions at either the acetyl-end or amide-end peptide site, one can get far more detailed information on the conditional probability of finding one site (either acetyl- or amide-end peptide) with N_{Ac} (N_{Am}) H-bonded solvent molecules when the other site is occupied by N_{Am} (N_{Ac}) H-bonded solvent molecules. We thus analyzed the MD trajectories further and measured the relative populations of [N_{Ac}, N_{Am}]$_{solvent}$ species.

Here, N_{Ac} (N_{Am}) is the number of solvent molecules H-bonded to the acetyl (amide)-end carbonyl oxygen atom. In Table 4, the populations of [N_{Ac}, N_{Am}]$_{solvent}$ species for the four solutions are summarized.

First of all, let us consider the AP−D$_2$O solution. The probability of finding [2, 2]$_{D_2O}$ species in the trans-AP−D$_2$O solution is the largest and is about 38.4%, whereas those of [1, 1]$_{D_2O}$ and [0, 0]$_{D_2O}$ are about 12.8% and 0.0%, respectively. What is interesting here is that the probability of finding [2, 1]$_{D_2O}$ species, 28.5%, is much larger than that of finding [1, 2]$_{D_2O}$ species, 17.2%. This means that, even though the total number of D$_2$O molecules H-bonded to trans-AP is commonly three for these two species, i.e., [2, 1]$_{D_2O}$ and [1, 2]$_{D_2O}$, the acetyl-end peptide has a large propensity of forming the second H-bond. The cis-AP also shows the same pattern. Nevertheless, it should be emphasized that the most probable species in the trans-AP−D$_2$O solution is [2, 2]$_{D_2O}$, 38.4%, where each of two peptides fully H-bonds to two water molecules. For the sake of comparison, we calculated the average number of D$_2$O molecules H-bonded to the acetyl- and amide-end peptides and found that $\bar{N}_{Ac} = 1.68$ and $\bar{N}_{Am} = 1.54$ for trans-AP and $\bar{N}_{Ac} = 1.68$ and $\bar{N}_{Am} = 1.48$ for cis-AP.

We next consider the cases of MeOD, EtOD, and PrOD solutions. For trans-AP in MeOD, the species having the largest population is [1, 1]$_{MeOD}$, 50.6%, whereas the probabilities of finding [0, 0]$_{MeOD}$ and [2, 2]$_{MeOD}$ are just about 1.3% and 2.2%, respectively, and are negligibly smaller than that of [1, 1]$_{MeOD}$. Also, the MD simulation shows that the population of [1, 0]$_{MeOD}$, 15.2%, is about three times larger than that of [0, 1]$_{MeOD}$, 4.4%, indicating that the acetyl-end peptide tends to form stronger H-bonds with MeOD molecules than the amide-end peptide does. This result is consistent with the case of the D$_2$O solution, though the absolute number of H-bonded MeOD molecules is far smaller than that of H-bonded D$_2$O molecules. The populations of [N_{Ac}, N_{Am}]$_{EtOD}$ and [N_{Ac}, N_{Am}]$_{PrOD}$ are quantitatively similar to those of [N_{Ac}, N_{Am}]$_{MeOD}$. In summary, the average numbers of solvent molecules H-bonded to the two sites of trans-AP are $\bar{N}_{Ac} = 1.13$ and $\bar{N}_{Am} = 0.90$ in MeOD, $\bar{N}_{Ac} = 1.10$ and $\bar{N}_{Am} = 0.94$ in EtOD, and $\bar{N}_{Ac} = 1.10$ and $\bar{N}_{Am} = 0.93$ in PrOD. These numbers are significantly smaller than those for trans-AP in D$_2$O.

In the present subsection, we have analyzed the MD trajectories of AP in various protic solvents and presented the detailed picture on the equilibrium H-bonding interaction of solvents only with the two carbonyl oxygen atoms of the AP peptide. However, the free amide group, ND$_2$, is another H-bonding site, and its interaction with solvent hydroxyl groups can play a role in determining the solution structure of AP. It turns out that the average numbers of solvent molecules H-bonded to the ND$_2$ group of trans-AP (cis-AP) in respective D$_2$O, MeOD, EtOD, and PrOD solutions are 0.52 (0.53), 0.44 (0.49), 0.33 (0.40), and 0.37 (0.34), all of which are significantly less than 1. Thus, it is believed that the H-bonding interaction of solvent OD groups with ND$_2$ might be less important than that with the carbonyl oxygen atoms.

From now on, we shall address the following critical questions. Can these theoretically predicted H-bonding patterns be confirmed by carrying out IR and VCD spectroscopic measurements of AP in these solutions? Is it possible to measure the site-specific H-bonding probability experimentally? If possible, are the present MD simulation results on the H-bond population distribution quantitatively in agreement with experimental findings? Bearing these questions in mind, we will present detailed analysis results on experimentally measured
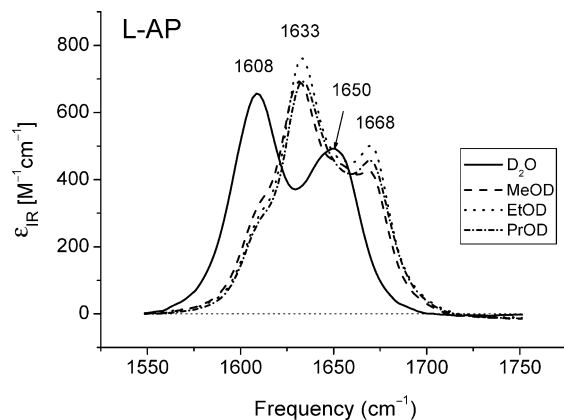
Figure 5. Experimentally measured IR absorption spectra of about 50 mg/mL L-AP in various protic solvents at 10 °C. See experimental details in section II.

spectra and directly compare them with the above MD simulation results in the following section.

IV. Experimental Results, Interpretations, And Discussions

A. Experimental Observations: IR Spectroscopy. The IR spectra of L-AP in protic solvents are all plotted in Figure 5 for the sake of comparison. The two major bands are associated with the amide I vibrations largely localized on the acetyl-end and amide-end peptides. Unlike L-AP in water (see the solid curve in Figure 5), however, L-AP in alcohol solutions (dashed/dotted curves) exhibits multiple peaks in IR spectra.

Water Solution. A detailed discussion on the amide I IR and VCD spectra of L-AP in D_2O was already presented in ref 1. However, for the sake of direct comparisons of the AP−D_2O spectra with those of the other solutions, we provide some new analysis results on the amide I IR spectrum of the AP−D_2O system. From the second-derivative spectrum (see Figure 6a upper), one can find two major components that are associated with the acetyl-end and amide-end amide I modes, denoted Ac1 and Am1. Performing a multipeak fitting with two Gaussian functions to the amide I IR band (Figure 6a lower), we found that the two components Ac1 and Am1 have center frequencies of 1608 and 1650 cm^{-1}, respectively (Table 5). The widths of these two fitted Gaussian functions are both 28 cm^{-1}, which is much larger than the typical lifetime broadening factor of about 5 cm^{-1}. This indicates (1) that the solvation dynamics and inhomogeneity of local solvent environments are the dominant factor in the amide I line broadening process and (2) that the local solvation dynamics and structural inhomogeneity around the acetyl- and amide-end peptides are quite close to each other, even though the H-bond populations at the two peptide sites differ from each other. The relative areas of these two peaks are 0.56 and 0.44, which correspond to the relative magnitudes of the two dipole strengths. This is based on the assumption that the two modes are not strongly coupled.

From the MD simulation trajectory of the AP−D_2O system in section III. C, we found that the average numbers of water molecules H-bonded to both acetyl- and amide-end carbonyl oxygen atoms are about 1.68 and 1.54, respectively. This result means that each of the two carbonyl oxygen atoms is always solvated (hydrated) by at least one or two water molecules. Consequently, the two bands associated with Ac1 and Am1 will be considered to be the fully solvated acetyl-end and amide-end amide I modes throughout this paper.

Methanol Solution. The IR spectrum of L-AP in MeOD (see the dashed curve in Figure 5) is notably different from that in

D_2O. Nevertheless, the overall amide I spectrum consists of two major peaks that are associated with the two amide I modes localized on the acetyl- and amide-end peptides, respectively. However, the two peak frequencies in MeOD are blue-shifted by about 25 cm^{-1} in comparison to those in D_2O, indicating that the average number of H-bonds formed by each carbonyl oxygen atom with MeOD is much smaller than that with D_2O molecules. In fact, the amide I frequency shift of 25 cm^{-1}, which is the frequency difference between the low-frequency peaks of the AP−D_2O and AP−MeOD solution spectra, can be typically induced by one or two H-bonding interactions of an amide carbonyl group with H-bond donors.[34] In addition to the frequency blue shifts, there appear complicated underlying features in the amide I IR band of L-AP in MeOD. To quantitatively determine detailed H-bonding statistics and to estimate how many bands contribute to each amide I band, we first calculated the second-derivative spectrum (see Figure 6b upper). It clearly shows that there are four spectral components under the amide I band. Thus, by using four Gaussian functions to fit the IR spectrum (Figure 6b lower), each spectral component can be identified (Table 5). The four peak frequencies are 1616, 1633, 1648, and 1668 cm^{-1}, respectively. Their relative areas are estimated to be 0.32, 0.24, 0.10, and 0.34, respectively. The first two (low-frequency) peaks, denoted Ac1 and Ac2, are associated with the amide I vibration of the acetyl-end peptide group, and it is believed that the two simply differ from each other by the number of methanol molecules H-bonded to the acetyl-end C=O group. The Ac1 component in the AP-MeOD spectrum is similar to that in the AP−D_2O spectrum, since they have similar frequencies and spectral line widths (∼28 cm^{-1}). Therefore, it is possible to assign this Ac1 component in both AP−MeOD and AP−D_2O spectra to be the amide I mode of the acetyl-end peptide with strongly hydrogen-bonded solvent molecules, either D_2O or MeOD. On the other hand, the second component, Ac2, is blue-shifted by 17 cm^{-1} from the Ac1 band in the AP−MeOD spectrum (see Table 5). Therefore, the Ac2 mode corresponds to the amide I mode of the acetyl-end peptide with fewer H-bonded solvent molecules in comparison to the Ac1 mode. The relative areas of Ac1 and Ac2 bands are 1.33:1 (= 0.32:0.24), suggesting that the relative population of the strongly H-bonded acetyl-end carbonyl group is larger than that of the less H-bonded acetyl-end carbonyl group. Here, it should be noted that the relative area of each underlying band is assumed to be proportional to the population of the corresponding H-bonding species. This is based on the more fundamental assumption that the dipole strength does not strongly depend on the local solvation environment. However, it was found that the dipole strength of NMA (*N*-methylacetamide)−water clusters has approximately 10−20% deviation, which reflects the inhomogeneity of local solvent environments.[35] Therefore, the assumption used in the present analysis is correct within such an error range.

Now, the two high-frequency bands, denoted Am1 and Am2, are associated with the amide I mode of the amide-end peptide group. The frequency difference between the Am1 and Am2 modes is about 20 cm^{-1}. Therefore, similar to the cases of Ac1 and Ac2 modes, the two modes Am1 and Am2 can be attributed to the amide I mode of the amide-end peptide with strongly H-bonded MeOD molecules and to that with less H-bonded MeOD molecules, respectively. The relative areas of Am1 and Am2 bands are found to be 1:3.4 (= 0.10:0.34). This observation suggests that the population of the amide-end peptide with fewer H-bonded MeOD molecules is larger than that with one or two H-bonded MeOD molecules. From these analyses, we reach the
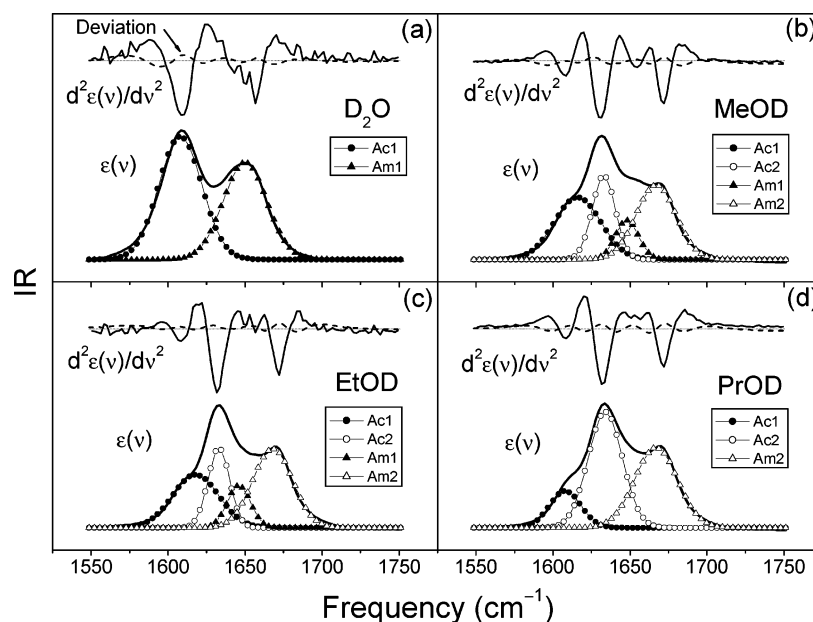
Figure 6. IR absorption (lower, $\epsilon(\nu)$) and their second derivative (upper, $d^2\epsilon(\nu)/d\nu^2$) spectra of L-AP in protic solvents. For quantitative comparison, IR absorption and second-derivative spectra are normalized. The curves under the amide I IR absorption band correspond to the fitted Gaussian functions. The center frequencies, areas, and widths of these Gaussian functions are summarized in Table 5. The deviation of the multiple-Gaussian fitted curve from the experimentally measured spectrum is plotted in the upper part of each figure (see the dashed curve).

TABLE 5: Multiple Gaussian Fittings to Experimentally Measured IR Absorption Spectra of L-AP in D$_2$O, MeOD, EtOD, and PrOD as Shown in Figure 6[a]

	acetyl-end amide I mode		amide-end amide I mode	
		D$_2$O		
components	Ac1	Ac2	Am1	Am2
frequency	1608		1650	
width	28		28	
area	0.56		0.44	
		MeOD		
components	Ac1	Ac2	Am1	Am2
frequency	1616	1633	1648	1668
width	29	15	14	25
area	0.32	0.24	0.10	0.34
		EtOD		
components	Ac1	Ac2	Am1	Am2
frequency	1618	1633	1646	1668
width	30	14	15	26
area	0.29	0.21	0.12	0.38
		PrOD		
components	Ac1	Ac2	Am1	Am2
frequency	1608	1634		1668
width	20	22		28
area	0.14	0.46		0.40

[a] Frequency and width in cm^{-1}. Area is normalized.

conclusion that the amide-end peptide group is less exposed to the H-bonding MeOD molecules than the acetyl-end peptide group is. This finding is quite consistent with the MD simulation results discussed in section III. C.

Nevertheless, the overall intensity (area) ratio of the acetyl-end (Ac1 + Ac2) to the amide-end (Am1 + Am2) amide I modes in AP−MeOD is still 0.56:0.44, which is identical to the case of AP−D$_2$O. This led us to believe that the transition dipole amplitudes of the two amide I modes do not change much when the solvent D$_2$O is replaced with MeOD.

Ethanol Solution. The IR spectrum of L-AP in EtOD (see the dotted curve in Figure 5) is quantitatively similar to that in MeOD. From the second-derivative spectrum (see Figure 6c upper), one can also find four underlying components. The multi-Gaussian fitting result is shown in Figure 6c lower and some characteristic values are summarized in Table 5. The four peak frequencies (areas) are found to be 1618 (0.29), 1633 (0.21), 1646 (0.12), and 1668 (0.38) cm^{-1}, respectively. Comparing these values with those of the AP−MeOD spectrum, we find that the two low-frequency components, Ac1 and Ac2, of the AP−EtOD directly correspond to those of AP−MeOD. Not only the peak frequencies but also the spectral bandwidths are similar in these two solutions. The only minor difference is that the Ac1 peak area of AP−EtOD is a bit smaller than that of AP−MeOD, indicating that the relative population of the acetyl-end peptide with strongly H-bonded EtOD molecules decreases slightly. This weakening of the H-bonding interaction of EtOD in comparison to MeOD can be attributed to the steric effect.

The two high-frequency components, Am1 and Am2, of the AP−EtOD spectrum are nearly identical to the corresponding ones of the AP−MeOD spectrum. Again, the population of the amide-end peptide with fewer H-bonded EtOD molecules is larger than that with one or two H-bonded EtOD molecules. It is quite interesting to note that the detailed band shape analysis results for the AP−EtOD spectrum are quantitatively similar to those for the AP−MeOD spectrum. This experimental finding is in good agreement with the MD simulation result of section III. C on the H-bond population distributions in the AP−MeOD and AP−EtOD systems.

Propanol Solution. Propanol has obviously the largest aliphatic side chain among the protic solvents considered in this paper. Therefore, one can expect the strongest steric effect on the hydrogen-bonding interactions of PrOD molecules with the two peptides. From the second-derivative spectrum (see Figure 6d upper), we could find only three spectral components. The multi-Gaussian fitting result is shown in Figure 6d lower, and some characteristic values are summarized in Table 5. The two low-frequency peaks can be assigned to the Ac1 and Ac2 modes,

since their frequencies are fairly close to those of the other alcohol solutions. However, it should be noted that the relative area of the Ac1 band is far smaller than that of Ac2. This suggests that the acetyl-end peptide with one or fewer H-bonded PrOD molecules is the dominant species, demonstrating the important role of the steric effect.

Also, the same trend can be seen in the amide-end peak too. The third component with the center frequency of 1668 cm^{-1} has to be assigned to the Am2 mode instead of the Am1 mode; note that the Am2 mode corresponds to the amide I mode of the amide-end C=O group that is relatively free from any H-bonding interaction with solvent PrOD molecules compared to the case of the Am1 mode. In the second-derivative spectrum in Figure 6d upper, there appears no additional amide-end amide I component with frequency smaller than 1668 cm^{-1}. Consequently, in the propanol solution of the AP dipeptide, the amide-end C=O group can hardly form two H-bonds with solvent PrOD molecules.

B. Equilibrium H-Bond Distribution: Experimental Analyses. From the detailed amide I band shape analyses of AP in protic solvents, one can see a gradual decrease in the population of acetyl-end C=O with two H-bonded solvent molecules by examining the areas of Ac1 components in the four amide I spectra. From D$_2$O to PrOD, these values (areas of Ac1 subband, see Table 5) are 0.56, 0.32, 0.29, and 0.14, respectively, indicating that the relative population of AP molecules with two H-bonded protic solvent molecules decreases as the solvent size increases. This experimental observation is consistent with the MD simulation result on the population distribution of the acetyl-end peptide with two H-bonded solvent molecules (see Figure 4a). In addition, the same pattern can be seen for the amide-end peptide by examining the area of the Am1 band (see Table 5), which varies from 0.44, 0.10, 0.12, to 0 as the solvent changes from D$_2$O, MeOD, EtOD, to PrOD. Again, this experimental observation agrees with the MD simulation analysis result on the population distribution of the amide-end peptide with two H-bonded solvent molecules in Figure 4b. Thus, the importance of the steric effect on the H-bonding interaction of protic solvents with a peptide group is experimentally proven.

Now, let us examine the distribution of H-bonded solvent molecules at each individual peptide site in detail. Within the limitation of factor analysis with Gaussian fitting to the experimentally measured IR spectrum, we find that the area of Ac1 band is approximately equal to that of Ac2 band in the cases of both MeOD and EtOD solutions (see Table 5). This experimental finding suggests that the population distributions of N_{Ac} in AP–MeOD and AP–EtOD solutions are likely to be symmetric. In contrast to the case of the acetyl-end peptide, the area of Am1 subband, which is associated with the amide-end peptide with strongly H-bonded solvent MeOD or EtOD molecules, is much smaller than that of Am2 band (see Table 5). More specifically, the ratio of the Am1 to Am2 band areas is about 1:3 for both MeOD and EtOD solutions. This experimental observation is clear evidence that the distribution of N_{Am} is asymmetric around $N_{Am} = 1$ and shifted toward $N_{Am} = 0$ region. Such asymmetric distributions of N_{Am} in the MeOD and EtOD solutions were already found in our MD trajectory analysis (Figure 4b), even though the experimentally estimated ratio of 1:3 could not be reproduced by the MD trajectory analyses. Finally, let us consider the PrOD solution. The Ac2 band area in the AP–PrOD IR spectrum is almost 3 times larger than the Ac1 band area (see Table 5). Again, this is a signature that the distribution of N_{Ac} is asymmetric around
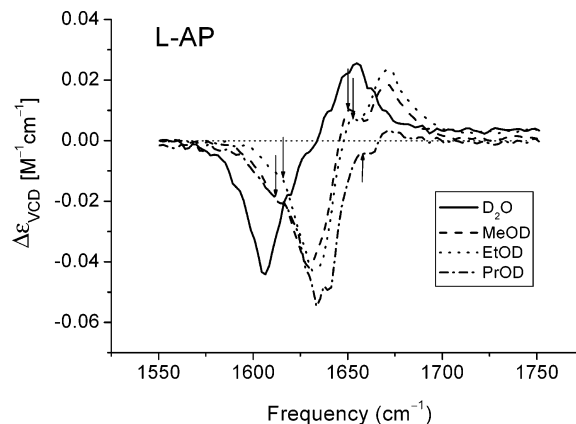
Figure 7. Experimentally measured VCD spectra of about 50 mg/mL L-AP in various protic solvents at 10 °C. See experimental details in section II. Although the signal to noise (*S/N*) ratio of the VCD spectrum is relatively small, the center frequencies of the VCD shoulder peaks indicated by arrows are found to be in good agreement with those of the (large *S/N* ratio) IR shoulder peaks.

$N_{Ac} = 1$ and shifted toward $N_{Ac} = 0$, whereas the MD simulation (Figure 4a) does not support this specific experimental finding; note that the H-bond population distribution in the AP–PrOD solution is quantitatively similar to those in the AP–MeOD and AP–EtOD solutions. From the factor analysis of the AP–PrOD spectrum, we found no contribution from the Am1 band, which indicates that the amide-end peptide predominantly forms a single H-bond with a PrOD molecule at a given time.

At the end of section III. C, a few questions were raised after the MD simulation trajectories had been fully analyzed to obtain the detailed H-bond population distributions around the two peptides of AP in protic solvents. Now, from the comparative investigations of the MD simulation and experimental analyses, it is believed that the answers to those questions were partly presented in this subsection. However, there is yet another issue about the solvent effect on the AP conformation in solution. Despite that the IR spectroscopy was found to be useful in extracting detailed information on the H-bond distribution, the overall shapes of amide I bands are similar for AP in protic solvents (see Figure 5). Thus, the VCD spectroscopy, which is presumably a better tool for such a purpose, is used to address the issue on the AP conformation in solutions.

C. Experimental Observations: VCD Spectroscopy. In Figure 7, we plot the total VCD spectra of L-AP in protic solvents including that in D$_2$O presented in ref 1. There are a few notable differences in these series of VCD spectra. First of all, the amide I VCD bands of AP in alcohol solutions are blue-shifted in comparison to that in D$_2$O. This was already discussed in the above section IV. A. Second, all VCD spectra exhibit the same negative–positive couplet pattern for the low–high frequency peak, indicating that the 3D solution structure of AP does not dramatically change as the solvent changes from water to the other alcohols. This is one of the most interesting observations in this paper, because it suggests that the hydrogen bond network-forming ability of solvent molecules does not make a significant difference in the solution structures of AP in these protic solvents. By noting that the AP structure in liquid D$_2$O was found to be close to the P$_{II}$ conformation, it becomes possible to speculate that the solution structure of AP in alcohol solutions considered in this paper is also similar to that in D$_2$O, i.e., P$_{II}$ conformation.

Nevertheless, the relative amplitude ratio of the negative (low-frequency) to positive (high-frequency) VCD peak progressively changes from AP–D$_2$O, AP–MeOD, AP–EtOD, to AP–PrOD

Site-Specific H-Bonding Interaction

J. Phys. Chem. A, Vol. 110, No. 50, 2006 **13363**
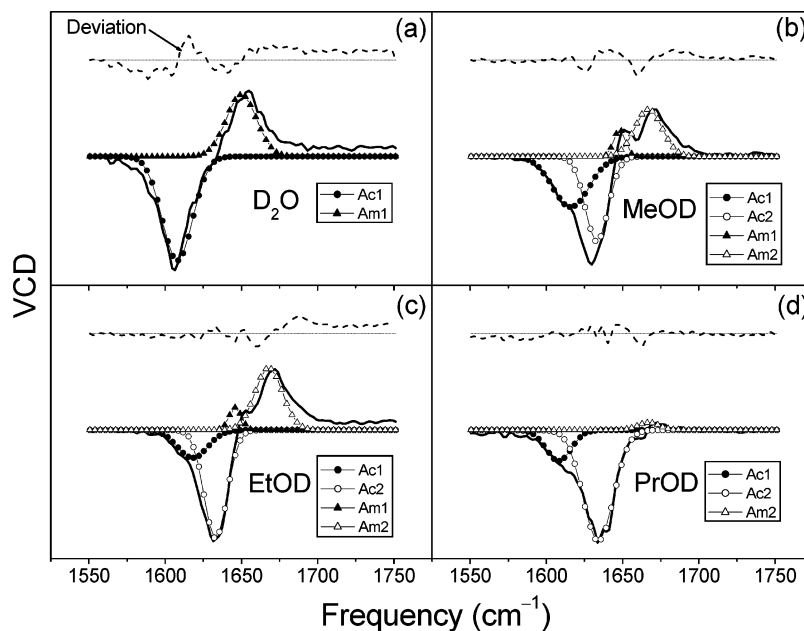
Figure 8. Factor analyses of VCD spectra of L-AP in protic solvents. For quantitative comparison, VCD spectra are normalized. The curves under the amide I VCD spectra are the fitted Gaussian functions. For quantitatively detailed information, see Table 6. The deviation of the multiple-Gaussian fitted curve from the experimentally measured spectrum is plotted in the upper part of each figure (see the dashed curve).

solutions, i.e., 1:0.59, 1:0.42, 1:0.59, and 1:0.04, respectively. More specifically, the rotational strength of the high-frequency amide-end mode comparatively decreases as the solvent size increases from D_2O, MeOD, EtOD, to PrOD. To find the relationship between this VCD line shape change and solution structural transition, we used the quantum chemistry calculation results on the rotational strengths of two AP amide I modes, which were presented in ref 1 (see the Supporting Information of ref 1). From the full contour maps of the rotational strengths with respect to the two dihedral angles ϕ and ψ, it is believed that the ensemble-averaged structure of AP varies from a P_{II}-like conformation in D_2O to some other conformation that lies between P_{II} and C_7 conformations in PrOD. However, this conclusion is slightly inconsistent with the MD simulation results. As can be seen in Figure 3, the MD simulation with the *ff*03 force field suggested that the ensemble-averaged conformation of AP is little dependent on solvents as long as the solvent is protic. Perhaps, this discrepancy between experiment and MD simulation shows the shortcomings of the currently available force field parameters.

D. Factor Analyses of VCD Spectra. In addition to the overall negative−positive couplet patterns of the measured VCD spectra, one can also identify multiple peak signatures in the VCD spectra of L-AP in alcohol solutions (see shoulder peaks and frequency-resolved peaks pointed by arrows in Figure 7). These underlying bands directly correspond to the multiple Gaussian components used to fit to the amide I IR absorption spectra. Using the same center frequencies for the Gaussian functions (in Table 5) and considering the weighting factors (areas) and spectral line widths to be the variational parameters, we carried out multiple-peak analyses for the VCD spectra. The fitting results are plotted in Figure 8 and summarized in Table 6.

Interestingly, the line widths of the fitted Gaussian peaks in VCD spectra are significantly smaller than those obtained by fitting to IR spectra (see Tables 5 and 6). To explain the additional spectral narrowing phenomena found in these VCD spectra in comparison to the corresponding IR spectra, it should first be noted that the rotational strengths are much more

TABLE 6: Multiple Gaussian Fittings to Experimentally Measured VCD Spectra of L-AP in D_2O, MeOD, EtOD, and PrOD as Shown in Figure 8[a]

	acetyl-end amide I mode		amide-end amide I mode	
		D_2O		
components	Ac1	Ac2	Am1	Am2
frequency	1608		1650	
width	20		20	
area	−1.00		0.59	
		MeOD		
components	Ac1	Ac2	Am1	Am2
frequency	1616	1633	1648	1668
width	24	15	7.5	18
area	−0.49	−0.51	0.08	0.34
		EtOD		
components	Ac1	Ac2	Am1	Am2
frequency	1618	1633	1646	1668
width	20	15	8	18
area	−0.26	−0.74	0.08	0.51
		PrOD		
components	Ac1	Ac2	Am1	Am2
frequency	1608	1634		1668
width	16.6	20		14
area	−0.19	−0.81		0.04

[a] Frequency and width in cm^{-1}. Area is normalized.

strongly dependent on the dihedral angles, ϕ and ψ, than the dipole strengths are (see ref 36). As shown in Figure 7 of ref 36, the rotational strength of a given amide I normal mode is almost completely determined by the so-called cross term (see ref 36 for a more detailed discussion), which is associated with the vibrational coupling-induced transition magnetic dipole and is a highly sensitive function of ϕ and ψ. Now, just for the sake of simplicity, let us assume that the line broadening process can be described by the instantaneous normal mode (INM) picture. Following the discussion in ref 37, one can ap-

proximately write down the IR and VCD spectra as

$$I(\omega) \propto \Big\langle \sum_j D_j(\phi, \psi)\delta[\omega - \omega_j(\phi, \psi)] \Big\rangle \qquad (1)$$

$$\Delta I_{VCD}(\omega) \propto \Big\langle \sum_j R_j(\phi, \psi)\delta[\omega - \omega_j(\phi, \psi)] \Big\rangle \qquad (2)$$

where, for an instantaneous polypeptide conformation, D_j, R_j, and ω_j are the dipole strength, rotational strength, and angular frequency of the jth amide I normal mode, respectively. $\delta[\omega]$ is the Dirac δ function. The angle bracket in eqs 1 and 2 represents the ensemble average over all thermally populated conformations. It should be noted that not only D_j and R_j but also the amide I mode frequency ω_j in a given instantaneous conformation depends on ϕ and ψ. However, only the dipole strength D_j is weakly dependent on ϕ and ψ, so that eq 1 can be further approximated as

$$I(\omega) \propto D_0 \Big\langle \sum_j \delta[\omega - \omega_j(\phi, \psi)] \Big\rangle = D_0\rho(\omega) \qquad (3)$$

where D_0 and $\rho(\omega)$ are the average dipole strength of a single amide I local mode and (un-normalized) density of states. The approximate eq 3 shows that the width of the overall IR spectrum is determined by the width of the density of states, $\rho(\omega)$, which reflects inhomogeneous distribution of local solvation structures. In contrast, eq 2 shows that the VCD spectrum is given by a *weighted* (by the rotational strength) density of states so that it has to be narrower than the density of states itself. Only when the rotational strength does not depend on the dipeptide conformation at all, the line width of a given VCD band becomes identical to that of the corresponding IR band. In other words, the VCD spectroscopy does not sample the entire inhomogeneously distributed amide I frequencies, whereas the IR spectroscopy generally does in the cases of the amide I vibrations.

E. Comparison Between *N*-Methylacetamide and AP in Protic Solvents: H-Bond Structures. In the present paper, we have used both MD simulation and IR and VCD measurement methods to study the site-specific H-bonding interaction of AP with various protic solvents. In relation to this, we investigated the H-bonding dynamics of *N*-methylacetamide (NMA) in both D_2O and MeOD and showed that the recently developed 2D vibrational spectroscopy can provide useful information on the H-bond formation and dissociation rates.[26,27] In the case of the NMA−D_2O solution, it was found that the carbonyl oxygen of NMA can form H-bonds with almost two water molecules. In contrast, the NMA carbonyl group can make H-bonds with either one or two MeOD molecules. Due to the existence of these two different solvation structures of NMA in MeOD, the amide I IR band appears to be a doublet even though NMA has only one amide I vibrational mode. The IR frequency splitting of NMA in MeOD was found to be about 20 cm^{-1}, which corresponds to the frequency red shift induced by a single H-bonding interaction of the amide with a MeOD molecule. In the 2D IR spectrum, one could find the two diagonal peaks that are directly associated with these two peaks. In addition, it appears that cross-peaks and their intensities are time-dependent. It was shown that the time-evolution of the cross-peak intensity can provide direct information on the relaxation time constant, which is given by the H-bond formation and dissociation rate constants.

In contrast, on the basis of the computer simulation studies of AP in protic solvents and partly from the experimental analyses of the IR and VCD spectra, we found that the number

of H-bonds to the acetyl- and amide-end carbonyl oxygen atoms is smaller than 2 in the case of water solution and is close to 1 in the other cases of alcoholic solvents including MeOD. This result shows that, even for a small dipeptide such as AP, the local environment around a given carbonyl group is congested and less exposed to solvent molecules. Therefore, it is expected that the peptide carbonyl oxygen atom in even larger polypeptides and proteins, even though it can be on the surface of a given protein, cannot make two H-bonding interactions with water molecules. This result is also consistent with our recent MD simulation study of an alanine-based α-helix in liquid water,[38] where we found that the average number of water molecules H-bonded to the backbone carbonyl group is ≤1 (see Figure 2c in ref 38).

F. H-Bonding Effect on the AP Dipeptide Structure in Protic Solvents. We now go back to the issue on the role of protic solvents in determining the solution structure of a dipeptide. Recent experimental and simulation studies on the structure of alanine dipeptide all pointed out that the dominant conformer is the left-handed P_{II} in water.[4−8] As shown by Drozdov et al.,[24] the intramolecular steric (repulsive) interaction is the most responsible factor for such a conformational preference. Recently, we showed that the AP dipeptide also adopts the same P_{II} conformation in D_2O, even though it has no amide proton at the acetyl-end peptide bond.[1] This was suggested to be another piece of supporting evidence testifying to the importance of the steric hindrance between two peptide groups in the AP. Unlike the D_2O solvent, MeOD and other alcohols considered in this paper do not have an ability to form the well-defined H-bond network structure. Nevertheless, we found that the AP structure in these alcoholic solvents is again close to P_{II}. This led us to believe that the lack of the extensive solvent-assisted H-bond network around the AP does not make a significant difference in the dipeptide structure. Bearing this fact in mind, let us discuss the origin of the structure-determining factor for AP in these protic solvents.

Note that the energy-minimum structure of trans-AP in the gas phase was found to be C_7, because it has a single intramolecular H-bond between the acetyl-end C=O oxygen atom and the amide-end ND_2 D-atom.[14,15] We found that, on the basis of the B3LYP/6-311++G(d,p) calculation, the energy difference between C_7 and P_{II} is about 1.12 kJ/mol for trans-AP. When the AP is solvated by protic solvent molecules, the acetyl-end C=O oxygen atom can change the H-bond partner from the amide-end ND_2 D-atom to the solvent ROD D-atom. Thus, there is a competition between intra- and intermolecular H-bonding interactions for the acetyl-end C=O group. If the intramolecular H-bonding interaction wins over the latter, the AP favors C_7, whereas if the intermolecular H-bonding interaction dominates, the P_{II}-like conformation becomes stable. Pappu and co-workers suggested that the water molecules have a strong ability to reduce the intramolecular electrostatic interaction between the two peptides in a given dipeptide molecule.[24] Thus, the only remaining factor is the intramolecular van der Waals type repulsive interaction. Then, the dipeptide P_{II} conformation is likely to be the energy-minimum structure on the potential energy surface approximately determined by the intramolecular van der Waals interaction. However, this description based on the electrostatic screening effect by the water cannot be used to explain the fact that the AP structures in even MeOD and EtOD solvents are close to the P_{II} conformation. Note that the dielectric constants of water, methanol, ethanol, and propanol are 80, 33, 25, and 21, respectively.[39] Certainly, the microscopic charge screening effect cannot be simply described by the

Site-Specific H-Bonding Interaction

J. Phys. Chem. A, Vol. 110, No. 50, 2006 **13365**

macroscopic dielectric constant. Nevertheless, the dielectric constant of a given solvent is a good measure of the charge screening efficiency. From these comparative investigations, we now believe that the more plausible (alternative) explanation for these phenomena, i.e., the notable P_{II} propensity of small dipeptide in water and other small alcoholic solvents, can be found by examining the competing nature of the intra- and intermolecular H-bonding interactions mentioned above. As long as the solvent molecules can form strong H-bonds with the peptide, there is little chance that the dipeptide forms an intramolecular H-bond. Thus, the dipeptide prefers a conformation without significant intramolecular electrostatic interaction. Then, why is the VCD spectrum of AP in PrOD so different from those in D_2O, MeOD, and EtOD solvents? It is because the PrOD is too bulky to have a strong H-bonding interaction with the peptide; note again that the ratio of the Ac1 to Ac2 band areas is 1:3.3 (0.14:0.46; see Table 5). Thus, the intramolecular H-bonding interaction becomes significant in this case, which in turn appears in the measured VCD spectrum.

V. Summary

In this paper, we presented both MD simulation and IR and VCD measurement results on the AP dipeptide dissolved in various protic solvents. From the MD simulation trajectories, the population distributions of H-bonded solvent molecules around the two peptides in the AP were obtained. It was found that the two peptides have different solvation environments. The average numbers of solvent molecules H-bonded to the two peptides in the AP suggest that the order of H-bonding abilities of these protic solvents is $D_2O >$ MeOD $\approx$ EtOD $\approx$ PrOD. By carrying out the factor analyses of measured amide I IR absorption spectra, quantitative information on the H-bond population distributions around the two peptides of AP could be obtained and found to be in good agreement with MD simulation results. To study the H-bonding interaction-induced effects on the AP structure in protic solvents, we measured the VCD spectra of AP and found that the dominant AP conformations in D_2O, MeOD, and EtOD are very close to the P_{II} form. On the other hand, the AP structure in PrOD is slightly different from those in other alcoholic solutions, but it is believed that the actual structure of AP in PrOD does not significantly deviate from P_{II}. It is noteworthy that the P_{II} structure of AP is not affected by the hydrogen bond network-forming ability of protic solvents nor by the solvent polarity as long as they are protic solvents. Taken together, the site-specific hydrogen-bonding interaction between the dipeptide and protic solvents appears to be pivotal in determining the structure of AP in solutions.

Supporting Information Available: Numerically simulated VCD spectra of L-AP in D_2O, MeOD, EtOD, and PrOD. This material is available free of charge via the Internet at http://pubs.acs.org.

References and Notes

(1) Lee, K.-K.; Hahn, S.; Oh, K.-I.; Choi, J. S.; Joo, C.; Lee, H.; Han, H.; Cho, M. *J. Phys. Chem. B* **2006**, *110*, 18834.

(2) Duan, Y.; Wu, C.; Chowdhury, S.; Lee, M. C.; Xiong, G.; Zhang, W.; Yang, R.; Cieplak, P.; Luo, R.; Lee, T.; Caldwell, J.; Wang, J.; Kollman, P. *J. Comput. Chem.* **2003**, *24*, 1999.

(3) Case, D. A.; Darden, T. A.; Cheatham, T. E., III; Simmerling, C. L.; Wang, J.; Duke, R. E.; Luo, R.; Merz, K. M.; Wang, B.; Pearlman, D. A.; Crowley, M.; Brozell, S.; Tsui, V.; Gohlke, H.; Mongan, J.; Hornak, V.; Cui, G.; Beroza, P.; Schafmeister, C.; Caldwell, J. W.; Ross, W. S.; Kollman, P. A. *AMBER 8*; University of California: San Francisco, 2004.

(4) Kim, Y. S.; Wang, J.; Hochstrasser, R. M. *J. Phys. Chem. B* **2005**, *109*, 7511.

(5) Poon, C.-D.; Samulski, E. T.; Weise, C. F.; Weisshaar, J. C. *J. Am. Chem. Soc.* **2000**, *122*, 5642.

(6) Woutersen, S.; Hamm, P. *J. Chem. Phys.* **2001**, *114*, 2727.

(7) Schweitzer-Stenner, R. *Biophys. J.* **2002**, *83*, 523.

(8) Madison, V.; Kopple, K. D. *J. Am. Chem. Soc.* **1980**, *102*, 4855.

(9) Vargas, R.; Garza, J.; Hay, B. P.; Dixon, D. A. *J. Phys. Chem. A* **2002**, *106*, 3213.

(10) Neria, E.; Fischer, S.; Karplus, M. *J. Chem. Phys.* **1996**, *105*, 1902.

(11) Wei, D.; Guo, H.; Salahub, D. R. *Phys. Rev. E* **2001**, *64*, 011907.

(12) Dadarlat, V. M. *Biophys. J.* **2005**, *89*, 1433.

(13) Hu, H.; Elstner, M.; Hermans, J. *Proteins* **2003**, *50*, 451.

(14) Hahn, S.; Lee, H.; Cho, M. *J. Chem. Phys.* **2004**, *121*, 1849.

(15) Wang, Z.-X.; Duan, Y. *J. Comput. Chem.* **2004**, *25*, 1699.

(16) Krimm, S.; Bandekar, J. *Adv. Protein Chem.* **1986**, *38*, 181.

(17) Pappu, R. V.; Rose, G. D. *Protein Sci.* **2002**, *11*, 2437.

(18) Chi, Z.; Chen, X. G.; Holtz, J. S. W.; Asher, S. A. *Biochemistry* **1998**, *37*, 2854.

(19) Moran, A.; Mukamel, S. *Proc. Natl. Acad. Sci. U.S.A.* **2004**, *101*, 506.

(20) Kubelka, J.; Keiderling, T. A. *J. Am. Chem. Soc.* **2001**, *123*, 12048.

(21) Hugosson, H. W.; Laio, A.; Maurer, P.; Rothlisberger, U. *J. Comput. Chem.* **2006**, *27*, 672.

(22) Mu, Y.; Stock, G. *J. Phys. Chem. B* **2002**, *106*, 5294.

(23) Han, W.-G.; Jalkanen, K. J.; Elstner, M.; Suhai, S. *J. Phys. Chem. B* **1998**, *102*, 2587.

(24) Drozdov, A. N.; Grossfield, A.; Pappu, R. V. *J. Am. Chem. Soc.* **2004**, *126*, 2574.

(25) Ge, N.-H.; Hochstrasser, R. M. *PhysChemComm* **2002**, *5*, 17.

(26) Kwac, K.; Cho, M. *J. Chem. Phys.* **2003**, *119*, 2247.

(27) Kwac, K.; Lee, H.; Cho, M. *J. Chem. Phys.* **2004**, *120*, 1477.

(28) Frisch, M. J.; Trucks, G. W.; Schlegel, H. B.; Scuseria, G. E.; Robb, M. A.; Cheeseman, J. R.; Montgomery, J. A., Jr.; Vreven, T.; Kudin, K. N.; Burant, J. C.; Millam, J. M.; Iyengar, S. S.; Tomasi, J.; Barone, V.; Mennucci, B.; Cossi, M.; Scalmani, G.; Rega, N.; Petersson, G. A.; Nakatsuji, H.; Hada, M.; Ehara, M.; Toyota, K.; Fukuda, R.; Hasegawa, J.; Ishida, M.; Nakajima, T.; Honda, Y.; Kitao, O.; Nakai, H.; Klene, M.; Li, X.; Knox, J. E.; Hratchian, H. P.; Cross, J. B.; Bakken, V.; Adamo, C.; Jaramillo, J.; Gomperts, R.; Stratmann, R. E.; Yazyev, O.; Austin, A. J.; Cammi, R.; Pomelli, C.; Ochterski, J. W.; Ayala, P. Y.; Morokuma, K.; Voth, G. A.; Salvador, P.; Dannenberg, J. J.; Zakrzewski, V. G.; Dapprich, S.; Daniels, A. D.; Strain, M. C.; Farkas, O.; Malick, D. K.; Rabuck, A. D.; Raghavachari, K.; Foresman, J. B.; Ortiz, J. V.; Cui, Q.; Baboul, A. G.; Clifford, S.; Cioslowski, J.; Stefanov, B. B.; Liu, G.; Liashenko, A.; Piskorz, P.; Komaromi, I.; Martin, R. L.; Fox, D. J.; Keith, T.; Al-Laham, M. A.; Peng, C. Y.; Nanayakkara, A.; Challacombe, M.; Gill, P. M. W.; Johnson, B.; Chen, W.; Wong, M. W.; Gonzalez, C.; Pople, J. A. *Gaussian 03*, revision C.02; Gaussian, Inc.: Wallingford, CT, 2004.

(29) Fox, T.; Kollman, P. A. *J. Phys. Chem. B* **1998**, *102*, 8070.

(30) Cornell, W. D.; Cieplak, P.; Bayly, C. I.; Gould, I. R.; Merz, K. M., Jr.; Ferguson, D. M.; Spellmeyer, D. C.; Fox, T.; Caldwell, J. W.; Kollman, P. A. *J. Am. Chem. Soc.* **1995**, *117*, 5179.

(31) Darden, T.; York, D.; Pederson, L. *J. Chem. Phys.* **1993**, *98*, 10089.

(32) Berendsen, H. J. C.; Postma, J. P. M.; van Gunsteren, W. F.; DiNola, A.; Haak, J. R. *J. Chem. Phys.* **1984**, *81*, 3684.

(33) Breneman, C. M.; Wiberg, K. B. *J. Comput. Chem.* **1990**, *11*, 361.

(34) Ham, S.; Kim, J.-H.; Lee, H.; Cho, M. *J. Chem. Phys.* **2003**, *118*, 3491.

(35) Bouř, P.; Keiderling, T. A. *J. Chem. Phys.* **2003**, *119*, 11253.

(36) Choi, J.-H.; Cho, M. *J. Chem. Phys.* **2004**, *120*, 4383.

(37) Hahn, S.; Ham, S.; Cho, M. *J. Phys. Chem. B* **2005**, *109*, 11789.

(38) Ham, S.; Hahn, S.; Lee, C.; Kim, T.-K.; Kwak, K.; Cho, M. *J. Phys. Chem. B* **2004**, *108*, 9333.

(39) *CRC Handbook of Chemistry and Physics*, 81st ed.; David, R. L., Ed.; CRC Press: New York, 2000−2001.